ENGN 2340 Final Project
Measuring the properties of hyperelastic materials

Daniel Gerbig

2013-12-13

Abstract

An iterative optimization method for measuring material properties that combines digital image correlation and the finite element method is applied to hyperelastic materials. The method is tested by measuring material properties for a neo-Hookean material loaded in uniaxial tension. Preliminary results show that the method can successfully measure material properties when given a suitable initial guess for the properties of interest.

1 Method for finding best-fit properties

Consider a tensile specimen of arbitrary geometry which is deformed by an external load of known magnitude. The displacement of a finite set of points on the surface of the specimen can be measured using a method like digital image correlation (DIC).

The deformation, in general, may be inhomogeneous. This prevents one from directly inferring the stress distribution from the loading imposed on the specimen. One method for determining the stress field is to perform a finite element simulation of the tensile test; unfortunately this requires *a priori* knowledge of the material properties which are currently unknown.

For a set of given of material properties, however, it is possible to compute the displacement field and external loads using a finite element simulation. These calculated quantities can then be compared to the experimentally observed displacement field and external load. The input material properties can then be refined so that they give finite element results that best-fit the observed experimental results.

To penalize differences between experiment and finite element simulations, define an objective function

$$\Pi = \frac{1}{2|\tilde{\mathbf{u}}|^2} \sum_{\Delta t} \int_S \left(\Delta\mathbf{u}(\mathbf{x}) - \Delta\tilde{\mathbf{u}}(\mathbf{x})\right) \cdot \left(\Delta\mathbf{u}(\mathbf{x}) - \Delta\tilde{\mathbf{u}}(\mathbf{x})\right) dA + \frac{1}{2|\tilde{\Phi}|^2} \sum_{\Delta t} \left(\Delta\Phi - \Delta\tilde{\Phi}\right)^2 \tag{1}$$

where $\mathbf{u}$ denotes the finite element displacement field, $\tilde{\mathbf{u}}$ denotes the experimental displacement field, Φ denotes the finite element stress power, $\tilde{\Phi}$ denotes the experimental stress power, and Δ denotes an increment of the aforementioned quantities during a time step Δt. The domain S that defines the bounds of integration is a surface on the experimental specimen where displacements are measured. In addition,

$$|\tilde{\mathbf{u}}|^2 = \sum_{\Delta t} \int_S \Delta\tilde{\mathbf{u}} \cdot \Delta\tilde{\mathbf{u}} dA \tag{2}$$

$$|\tilde{\Phi}|^2 = \sum_{\Delta t} \Delta\tilde{\Phi}^2 \tag{3}$$

are normalization factors. The best-fit material properties can be obtained by minimizing the objective function. This is done in an iterative fashion using the Newton-Raphson method. The correction dQ_β to material property Q_β can be solved for from the equation

$$\frac{\partial^2\Pi}{\partial Q_\alpha \partial Q_\beta} dQ_\beta = -\frac{\partial \Pi}{\partial Q_\alpha} \tag{4}$$

and then the material property can be corrected

$$Q_\beta^{n+1} = Q_\beta^n + dQ_\beta \tag{5}$$

where the superscript n and $n+1$ denote material properties at Newton-Raphson iteration n and $n+1$, respectively.

After introducing the usual finite element interpolations for the displacements, the necessary derivatives can be written as

$$\frac{\partial \Pi}{\partial Q_\alpha} = \frac{1}{|\tilde{\mathbf{u}}|^2}\sum_{\Delta t}\left(\mathbf{M}\Delta\mathbf{u} - \tilde{\mathbf{M}}\Delta\tilde{\mathbf{u}}\right)\cdot\mathbf{M}\mathbf{H}_\alpha + \frac{1}{|\tilde{\Phi}|^2}\sum_{\Delta t}\left[\left(\hat{\mathbf{K}}\mathbf{H}_\alpha - \mathbf{p}_\alpha\right)\cdot\Delta\mathbf{u} + \hat{\mathbf{R}}\cdot\mathbf{H}_\alpha\right]\left(\Delta\Phi - \Delta\tilde{\Phi}\right) \tag{6}$$

and

$$\begin{aligned}\frac{\partial^2 \Pi}{\partial Q_\alpha \partial Q_\beta} =& \frac{1}{|\tilde{\mathbf{u}}|^2}\sum_{\Delta t}\left[\mathbf{M}\mathbf{H}_\alpha\cdot\mathbf{M}\mathbf{H}_\beta + \left(\mathbf{M}\Delta\mathbf{u} - \tilde{\mathbf{M}}\Delta\tilde{\mathbf{u}}\right)\cdot\mathbf{M}\mathbf{H}_{\alpha\beta}\right] \\ &+ \frac{1}{|\tilde{\Phi}|^2}\sum_{\Delta t}\left[\left(\hat{\mathbf{K}}\mathbf{H}_\alpha - \mathbf{p}_\alpha\right)\cdot\Delta\mathbf{u} + \hat{\mathbf{R}}\cdot\mathbf{H}_\alpha\right]\left[\left(\hat{\mathbf{K}}\mathbf{H}_\beta - \mathbf{p}_\beta\right)\cdot\Delta\mathbf{u} + \hat{\mathbf{R}}\cdot\mathbf{H}_\beta\right] \\ &+ \frac{1}{|\tilde{\Phi}|^2}\sum_{\Delta t}\left[\left(\frac{\partial\hat{\mathbf{K}}}{\partial Q_\beta}\mathbf{H}_\alpha + \frac{\partial\hat{\mathbf{K}}}{\partial Q_\alpha}\mathbf{H}_\beta + \frac{\partial\hat{\mathbf{K}}}{\partial\mathbf{u}}\mathbf{H}_\beta\mathbf{H}_\alpha + \hat{\mathbf{K}}\mathbf{H}_{\alpha\beta} - \frac{\partial\mathbf{p}_\alpha}{\partial Q_\beta}\right)\cdot\Delta\mathbf{u}\right]\left(\Delta\Phi - \Delta\tilde{\Phi}\right) \\ &+ \frac{1}{|\tilde{\Phi}|^2}\sum_{\Delta t}\left[\left(\hat{\mathbf{K}}\mathbf{H}_\alpha - \mathbf{p}_\alpha\right)\cdot\mathbf{H}_\beta + \left(\hat{\mathbf{K}}\mathbf{H}_\beta - \mathbf{p}_\beta\right)\cdot\mathbf{H}_\alpha + \mathbf{R}\cdot\mathbf{H}_{\alpha\beta}\right]\left(\Delta\Phi - \Delta\tilde{\Phi}\right). \end{aligned} \tag{7}$$

where $\hat{\mathbf{K}}$ is the unconstrained finite element stiffness matrix, $\hat{\mathbf{R}}$ is the unconstrained finite element residual vector, $\mathbf{M}$ is the finite element mass matrix for the surface S, and $\tilde{\mathbf{M}}$ is the experimental mass matrix for the surface S. The vectors $\mathbf{H}_\alpha$ and $\mathbf{H}_{\alpha\beta}$ represent first and second derivatives of the displacement $\mathbf{u}$ with respect to material properties Q_α. They are calculated by solving the following systems of equations:

$$\mathbf{K}\mathbf{H}_\alpha = \mathbf{p}_\alpha \tag{8}$$

and

$$\mathbf{K}\mathbf{H}_{\alpha\beta} = \frac{\partial\mathbf{p}_\alpha}{\partial Q_\beta} - \frac{\partial\mathbf{K}}{\partial Q_\alpha}\mathbf{H}_\beta - \frac{\partial\mathbf{K}}{\partial Q_\beta}\mathbf{H}_\alpha - \frac{\partial\mathbf{K}}{\partial\mathbf{u}}\mathbf{H}_\beta\mathbf{H}_\alpha \tag{9}$$

where $\mathbf{p}_\alpha = -\partial\mathbf{R}/\partial Q_\alpha$ is the derivative of the constrained finite element residual vector, and $\mathbf{K}$ is the constrained finite element stiffness matrix.

Calculating $\mathbf{p}_\alpha$, $\partial\mathbf{p}_\alpha/\partial Q_\beta$, and $\partial\mathbf{K}/\partial Q_\alpha$ requires taking derivatives of the Kirchhoff stress τ_{ij}. The necessary derivatives are

$$\partial\tau_{ij}/\partial Q_\alpha \tag{10}$$

$$\partial^2\tau_{ij}/\partial Q_\alpha\partial Q_\beta \tag{11}$$

$$\partial C_{ijkl}/\partial Q_\alpha. \tag{12}$$

A common technique for implementing a nearly incompressible hyperelastic element in a finite element code is the F-bar method. This formulation increases the complexity of the the derivative $\partial\mathbf{K}/\partial\mathbf{u}$. Once implemented correctly, evaluating the derivative adds significant overhead to the computation of derivatives of Π (note that the derivative is a rank 6 tensor, though full use of symmetry should reduce the number of unique entries).

Because the derivation, implementation, validation, and computational cost of this particular derivative appears large, it is ignored. The optimization method will not be a true Newton-Raphson method, as the Hessian $\partial^2\Pi/\partial Q_\alpha\partial Q_\beta$ will be approximate, but instead will be a Quasi-Newton method.

2 Application to hyperelastic materials

With the framework for the optimization procedure already established, the focus of this investigation will be to implement the material model and the necessary derivatives in order to find best-fit properties for hyperelastic materials.

2.1 General hyperelastic material

Consider a hyperelastic material with a strain energy density $\bar{U}$. The strain energy density can be written as a function

$$\bar{U} = \bar{U}(\bar{I}_1, \bar{I}_2, J) \tag{13}$$

where $\bar{I}_1$, $\bar{I}_2$, and J are the invariants of the left Cauchy-Green deformation tensor $B_{ij} = F_{ik}F_{jk}$:

$$\bar{I}_1 = \frac{B_{kk}}{J^{2/3}} \tag{14}$$

$$\bar{I}_2 = \frac{1}{2}\left((\bar{I}_1)^2 - \frac{B_{ik}B_{ki}}{J^{4/3}}\right) \tag{15}$$

$$J = \sqrt{\det \mathbf{B}}. \tag{16}$$

Given a strain energy density of this form, the Cauchy stress σ_{ij} can be written as

$$\sigma_{ij} = \frac{2}{J}\left[\frac{1}{J^{2/3}}\left(\frac{\partial \bar{U}}{\partial \bar{I}_1} + \bar{I}_1 \frac{\partial \bar{U}}{\partial \bar{I}_2}\right)B_{ij} - \left(\bar{I}_1 \frac{\partial \bar{U}}{\partial \bar{I}_1} + 2\bar{I}_2 \frac{\partial \bar{U}}{\partial \bar{I}_2}\right)\frac{\delta_{ij}}{3} - \frac{1}{J^{4/3}}\frac{\partial \bar{U}}{\partial \bar{I}_2} B_{ik}B_{kj}\right] + \frac{\partial \bar{U}}{\partial J}\delta_{ij} \tag{17}$$

The finite element implementation of the material requires the Kirchhoff stress τ_{ij}, which is defined as

$$\tau_{ij} = J\sigma_{ij}. \tag{18}$$

The elastic stiffness C_{ijkl} is also needed; it can be calculated from the expression

$$C_{ijkl} = \frac{\partial \tau_{ij}}{\partial F_{km}} F_{lm}. \tag{19}$$

2.2 Application to a neo-Hookean material

The strain energy potential for a neo-Hookean material is

$$\bar{U} = \frac{\mu_1}{2}\left(\bar{I}_1 - 3\right) + \frac{K_1}{2}\left(J - 1\right)^2. \tag{20}$$

Combining this potential with equations 17 and 18 gives the following expression for the Kirchhoff stress:

$$\tau_{ij} = \frac{\mu_1}{J^{2/3}}\left(B_{ij} - \frac{B_{kk}}{3}\delta_{ij}\right) + K_1 J\left(J - 1\right)\delta_{ij}. \tag{21}$$

This expression can then be differentiated (cf. equation 19) to give the tangent stiffness

$$C_{ijkl} = \frac{\mu_1}{J^{2/3}}\left[\delta_{ik}B_{jl} + B_{il}\delta_{jk} - \frac{2}{3}\left(B_{ij}\delta_{kl} + B_{kl}\delta_{ij}\right) + \frac{2}{3}\frac{B_{qq}}{3}\delta_{ij}\delta_{kl}\right] + K_1\left(2J - 1\right)J\delta_{ij}\delta_{kl}. \tag{22}$$

These expressions can be then be differentiated with respect to Q_α to obtain the necessary derivatives (cf. equations 10 - 12) for the iterative property optimization. The results are as follows:

$$\frac{\partial \tau_{ij}}{\partial \mu_1} = \frac{1}{J^{2/3}} \left(B_{ij} - \frac{B_{kk}}{3} J \delta_{ij} \right) \tag{23}$$

$$\frac{\partial \tau_{ij}}{\partial K_1} = J \left(J - 1 \right) \delta_{ij} \tag{24}$$

$$\frac{\partial^2 \tau_{ij}}{\partial \mu_1^2} = 0 \tag{25}$$

$$\frac{\partial^2 \tau_{ij}}{\partial \mu_1 \partial K_1} = 0 \tag{26}$$

$$\frac{\partial^2 \tau_{ij}}{\partial K_1^2} = 0 \tag{27}$$

$$\frac{\partial C_{ijkl}}{\partial \mu_1} = \frac{1}{J^{2/3}} \left[\delta_{ik} B_{jl} + B_{il} \delta_{jk} - \frac{2}{3} \left(B_{ij} \delta_{kl} + B_{kl} \delta_{ij} \right) + \frac{2}{3} \frac{B_{qq}}{3} \delta_{ij} \delta_{kl} \right] \tag{28}$$

$$\frac{\partial C_{ijkl}}{\partial K_1} = \left(2J - 1 \right) J \delta_{ij} \delta_{kl}. \tag{29}$$

$$\tag{30}$$

3 Implementation and verification

3.1 Material

A hyperelastic neo-Hookean element was implemented in FEACHEAP. The element was verified using the "CHECK STIFFNESS" command in FEACHEAP and by comparing the results of stretching a single element to the Matlab code provided in the course programming notes.

3.2 Material derivatives

The derivatives in equations 10 - 12 were verified using numerical differentiation. The analytic first derivative of the Kirchhoff stress was verified against numerical derivatives of the Kirchhoff stress. Once the analytic first derivative agreed with the numerical first derivative, the analytic second derivative was verified; it was compared to the numerical derivative of the analytic first derivative. The analytic derivative of the material stiffness C_{ijkl} was verified against numerical derivatives of the material stiffness.

4 Model problem for testing the method

The boundary value problem used to test the iterative method was a simulation of a uniaxial tension test. The bar was arbitrarily assigned a gage length of 57, a gage width of 12.7, and a gage thickness of 4. The focus of the investigation is the performance of the iterative optimization procedure, so the physical units (nominally millimeters, to make the dimensions of the bar similar to standard tensile specimens) are of little interest.

The mesh of the tensile bar is shown below in figure 1. Symmetry boundary conditions were used reduce the model to one-eighth of the specimen. A displacement in the y-direction of $u_2 = 20$ was applied to the top face of the bar to simulate the pulling action of a test machine gripper. For simplicity the displacements in the x- and z-direction (u_1 and u_3, respectively) were fixed at zero. A plot of the deformed configuration of the tensile bar is shown in figure 2.

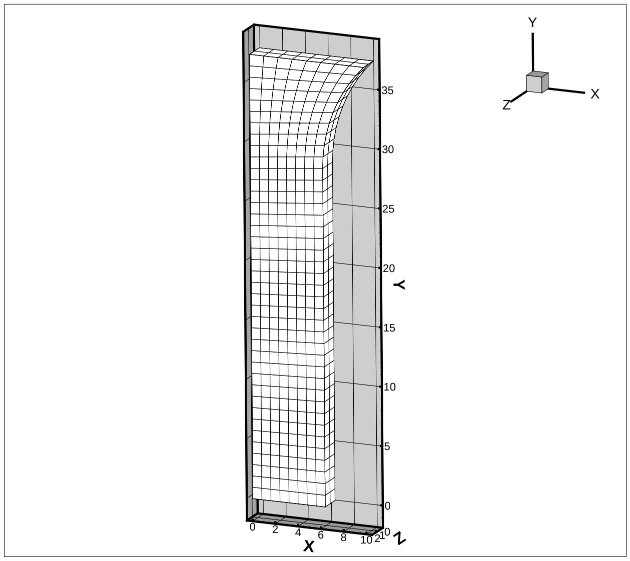

Figure 1: The reference configuration of the bar. Symmetry boundary conditions were applied to the three opposite faces of the bar to reduce the number of degrees of freedom.

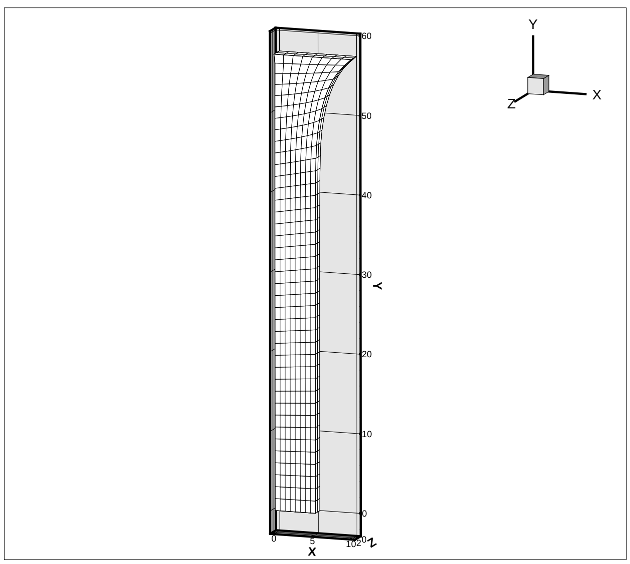

Figure 2: The deformed configuration of the bar after imposing a vertical displacement $u_2 = 20$ on the top face.

The general procedure for testing the optimization procedure is outlined below:

1. Choose target properties μ_1^*, K_1^* (giving an associated Poisson's ratio $\nu^* = (3K_1^* - 2\mu_1^*)/[3(K_1^* + \mu_1^*)]$) and generate a displacement and load history using a finite element simulation. This data will serve as the "experimental" data set.

2. Choose some initial guess for the material properties $\mu_1 \neq \mu_1^*$, $K_1 \neq K_1^*$.

3. Run the property optimization procedure to refine the guess properties. This will eventually recover

the best-fit properties to the experimental data. These best-fit properties should match the target properties used to generate the experimental data set.

The optimization procedure was tested using two sets of target properties. The first set of target properties was used to investigate a nearly incompressible material. The target properties used were $\mu_1^* = 1$ and $K_1^* = 10$, corresponding to a Poisson's ratio of $\nu = 0.45161$. The second set of target material properties was used to approach the fully incompressible limit. The target properties used were $\mu_1^* = 1$ and $K_1^* = 1000$. The corresponding Poisson's ratio for this set of properties is $\nu = 0.4995$.

Again, since the performance and robustness of the iterative optimization procedure is the primary concern of this investigation, the physical units for μ_1 and K_1 (nominally MPa) are of little importance.

5 Results

5.1 $\mu_1^* = 1, K_1^* = 10 \iff \nu^* = 0.45151$

The solution for a single initial guess will be analyzed to determine if the property optimization is working. The solution for each Newton-Raphson iteration for a guess of 10% of the target properties is summarized below in table 1. It is clear that the properties μ_1 and K_1 are quickly refined to best-fit properties that match the target properties.

Iteration	μ_1	K_1
1	0.100000	1.000000
2	0.968235	9.682360
3	0.998879	9.988788
4	0.999960	9.999613

Table 1: Best-fit material properties μ_1 and K_1 after each Newton-Raphson step in the optimization procedure. The optimization procedure was stopped after 4 iterations by a convergence criterion based on the norm of the Newton-Raphson correction.

It is also helpful to compare the load-displacement curve from the experimental data set with the load-displacement curve from the finite element simulation at each subsequent best-fit property iteration. This serves as a simple check to see how well the finite element solution reproduces the experimental results.

Consider the family of curves shown below in figure 3 for the series of iterations from table 1. The first Newton-Raphson iteration, shown in figure 3 (a), corresponds to the initial guess of 10% of the target properties. The finite element simulation with a low initial guess for μ_1 and K_1 resulted in a low load-displacement curve compared with experiment. The behavior from the second Newton-Raphson iteration is shown in figure 3 (b). At this iteration the corrected material properties are much closer to the target properties, making the finite element results nearly match the experimental results. By the third Newton-Raphson iteration (part (c)), the finite element and experimental load-displacement behaviors are indistinguishable. The behavior at the fourth Newton-Raphson iteration (part (d)) is identical to the third, indicating that the property optimization has converged.

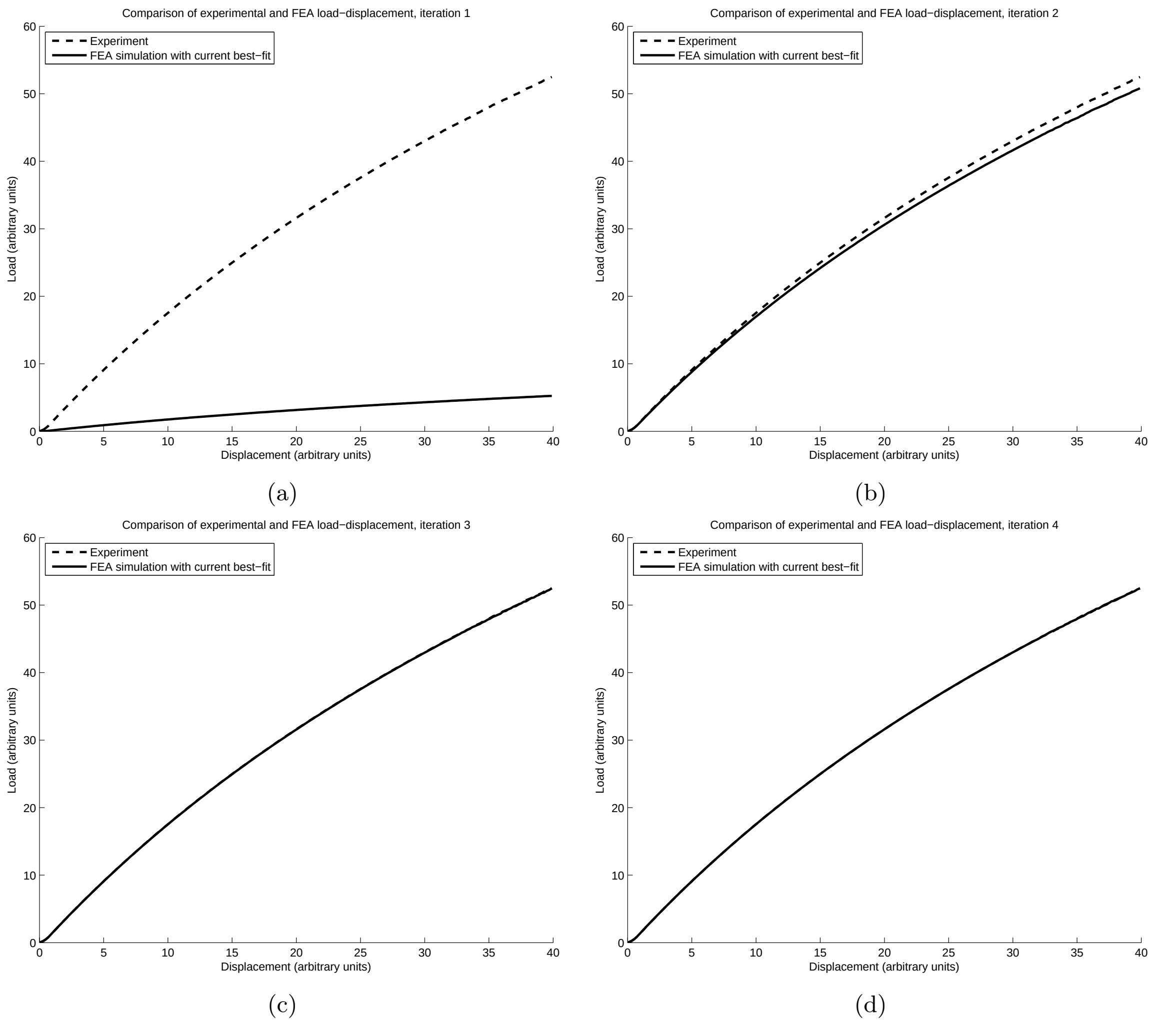

Figure 3: Comparison between the load-displacement curve from the experimental data set and the load-displacement curve from the finite element simulation using properties at each Newton-Raphson iteration.

Three different initial guesses were used to test the optimization procedure. Two initial guesses were able to recover the target properties as the best-fit material parameters. The other initial guess diverged to properties that caused excessive time step cutbacks when solving for equilibrium, eventually causing the finite element simulation to fail. The results of all three initial guesses are summarized below in table 2.

Test No.	μ_1	K_1	ν	Recovers target props.?	Notes
1	0.1	1	0.45161	Yes	4 Newton-Raphson iterations
2	0.1	100	0.49950	No	Failed after 21 Newton-Raphson iterations
3	10	100	0.45161	Yes	5 Newton-Raphson iterations

Table 2: Results of the iterative property optimization for three different initial guesses, for a nearly incompressible material.

5.2 $\mu_1^* = 1, K_1^* = 1000 \iff \nu^* = 0.49950$

Four different initial guesses were tested using the iterative property optimization procedure. The results of all four initial guesses are summarized below in table 3.

Test No.	μ_1	K_1	ν	Recovers target props.?	Notes
1	0.1	100	0.49950	Yes	3 Newton-Raphson iterations
2	0.1	10000	0.50000	Yes	158 Newton-Raphson iterations
3	10	100	0.45161	Yes	626 Newton-Raphson iterations
4	10	10000	0.49950	Yes	134 Newton-Raphson iterations

Table 3: Results of the iterative property optimization for four different initial guesses, for a fully incompressible material.

6 Discussion and Conclusions

The initial results of the property optimization procedure indicate that it is possible to find best-fit material parameters for a neo-Hookean material, in both the case of a nearly incompressible material and a fully incompressible material.

Unfortunately, the results also indicate that the optimization is sensitive to the initial guess for material properties. It may be necessary to implement a trust-region algorithm to appropriately accept or reject Newton-Raphson corrections for these cases.

Looking at tables 2 and 3 is is apparent that tests that were started with a Poisson's ratio different from the target value of ν^* observed the poorest convergence behavior (or failed to converge at all). In the case of the nearly incompressible material (table 2, test 2) the property optimization failed. In the case of the fully incompressible material (table 3, test 3) the optimization took an excessive number of Newton-Raphson steps. Conversely, initial guesses that had a Poisson's ratio identical with the target ν^* exhibited good convergence.

In the cases where the initial property guess has a Poisson's ratio identical to ν^*, the resulting finite element displacement field is identical to the experimental displacement field. As such, there is no contribution from the first term in the objective function given in equation 1. Contrast this with the cases where the initial property guess has a Poisson's ratio different from ν^*, where the finite element and experimental displacement fields do not agree, making the first term in the objective nonzero.

The correlation between poor convergence and a presence of differences in displacement fields suggests that it is the displacement penalty term that hurts the rate of convergence. The current formulation of this term penalizes differences in displacement fields on a surface of the specimen. A simple reformulation could be to penalize differences between displacement fields measured in a *volume* of the specimen (with experimental fields measured by digital volume correlation) instead of on a *surface*:

$$\Pi = \frac{1}{2|\tilde{\mathbf{u}}|^2} \sum_{\Delta t} \int_V (\Delta\mathbf{u}(\mathbf{x}) - \Delta\tilde{\mathbf{u}}(\mathbf{x})) \cdot (\Delta\mathbf{u}(\mathbf{x}) - \Delta\tilde{\mathbf{u}}(\mathbf{x}))\, dV + \frac{1}{2|\tilde{\Phi}|^2} \sum_{\Delta t} \left(\Delta\Phi - \Delta\tilde{\Phi}\right)^2. \tag{31}$$

This will allow the objective function to penalize differences between experimental and finite element deformations that are volumetric, which may help the rate of convergence for the property K_1. Further work will be done to determine how this modification affects the rate of convergence.